Biochimica et Biophysica Acta 1832 (2013) 2153–2161

Contents lists available at ScienceDirect

Biochimica et Biophysica Acta

journal homepage: www.elsevier.com/locate/bbadis

Combined molecular MRI and immuno-spin-trapping for in vivo detection of free radicals in orthotopic mouse GL261 gliomas

Rheal A. Towner [a,*], Nataliya Smith [a], Debra Saunders [a], Patricia Coutinho De Souza [a], Leah Henry [a,1], Florea Lupu [b], Robert Silasi-Mansat [b], Marilyn Ehrenshaft [c], Ronald P. Mason [c], Sandra E. Gomez-Mejiba [d], Dario C. Ramirez [d]

[a] Advanced Magnetic Resonance Center, Oklahoma Health Sciences Center, Oklahoma City, OK 73104, USA
[b] Cardiovascular Biology, Oklahoma Medical Research Foundation, Oklahoma City, OK 73104, USA
[c] Laboratory of Toxicology and Pharmacology, National Institute of Environmental Health Sciences, Research Triangle Park, NC 27709, USA
[d] Laboratory of Experimental Medicine & Therapeutics, Instituto Multidisciplinario de Investigaciones Biologicas-San Luis—CONICET-National University of San Luis, San Luis 5700, Argentina

ARTICLE INFO

Article history:
Received 15 April 2013
Received in revised form 5 July 2013
Accepted 12 August 2013
Available online 17 August 2013

Keywords:
Molecular magnetic resonance imaging
Glioma
Free radical
Immuno-spin-trapping
In vivo
Mouse

ABSTRACT

Free radicals play a major role in gliomas. By combining immuno-spin-trapping (IST) and molecular magnetic resonance imaging (mMRI), in vivo levels of free radicals were detected within mice bearing orthotopic GL261 gliomas. The nitrone spin trap DMPO (5,5-dimethyl pyrroline *N*-oxide) was administered prior to injection of an anti-DMPO probe (anti-DMPO antibody covalently bound to a bovine serum albumin (BSA)–Gd (gadolinium)-DTPA (diethylene triamine penta acetic acid)–biotin MRI contrast agent) to trap tumor-associated free radicals. mMRI detected the presence of anti-DMPO adducts by either a significant sustained increase ($p < 0.001$) in MR signal intensity or a significant decrease ($p < 0.001$) in T_1 relaxation, measured as $\%T_1$ change. In vitro assessment of the anti-DMPO probe indicated a significant decrease ($p < 0.0001$) in T_1 relaxation in GL261 cells that were oxidatively stressed with hydrogen peroxide, compared to controls. The biotin moiety of the anti-DMPO probe was targeted with fluorescently-labeled streptavidin to locate the anti-DMPO probe in excised brain tissues. As a negative control a non-specific IgG antibody covalently bound to the albumin–Gd-DTPA–biotin construct was used. DMPO adducts were also confirmed in tumor tissue from animals administered DMPO, compared to non-tumor brain tissue. GL261 gliomas were found to have significantly increased malondialdehyde (MDA) protein adducts ($p < 0.001$) and 3-nitrotyrosine (3-NT) ($p < 0.05$) compared to normal mouse brain tissue, indicating increased oxidized lipids and proteins, respectively. Co-localization of the anti-DMPO probe with either 3-NT or 4-hydroxynonenal was also observed. This is the first report regarding the detection of in vivo levels of free radicals from a glioma model.

1. Introduction

Reactive oxygen (and nitrogen) species (ROS/RNS) generated from oxidative stress play a crucial role in cancers such as gliomas, either as modulators of signal transduction or as a causal agent of tissue injury. Understanding the extent and timing of in vivo events triggered by free radicals is important to consider, as these are major determinants of disease evolution and progression. By combining molecular magnetic resonance imaging (mMRI) and immuno-spin trapping (IST) technologies it is possible for the first time to monitor levels of in vivo radicals in rodent glioma models.

Numerous studies indicate that oxidative stress, a result of an imbalance in levels of ROS/RNS and anti-oxidative defense systems, plays a crucial role in cancer. Free radicals are involved and/or are the causal agents in several cancers, including gliomas. ROS/RNS may directly oxidize nucleic acids, proteins, carbohydrates and lipids, causing intracellular and intercellular perturbations in homeostasis, including DNA mutations and interference with DNA repair [1]. High concentrations of lipid-derived electrophilic products resulting from the oxidation process readily react with proteins, DNA and phospholipids, generating intra- and intermolecular toxic covalent adducts that lead to the propagation and amplification of oxidative stress [1].

Abbreviations: Anti-DMPO probe, anti-DMPO antibody–albumin–Gd-DTPA–biotin; BSA, bovine serum albumin; EDC, N-succinimidyl 3-(2-pyridyldithio)-propionate; Gd-DTPA, gadolinium-diethylene triamine penta acetic acid; HN, 4-hydroxynonenal; IgG, immunoglobulin G; IgG contrast agent, IgG-albumin–Gd-DTPA–biotin; IHC, immunohistochemistry; IST, immuno-spin-trapping; DMPO, 5,5 dimethyl-1-pyrroline-*N*-oxide; MRI, magnetic resonance imaging; mMRI, molecular MRI; MDA, malondialedhyde; NHS, N-succinimidyl-S-acetylthioacetate; 3-NT, 3-nitrotyrosine; PBS, phosphate buffer saline; ROIs, regions of interest; ROS/RNS, reactive oxygen (nitrogen) species; TE, echo time; TR, repetition time

* Corresponding author. Tel.: +1 405 271 7383; fax: +1 405 271 7254.
E-mail addresses: Rheal-Towner@omrf.org (R.A. Towner), leah-henry@ouhsc.edu (L. Henry).
[1] Current address: College of Medicine, University of Oklahoma Health Sciences Center, Oklahoma City, OK 73104, USA.

0925-4439/$ – see front matter © 2013 Elsevier B.V. All rights reserved.
http://dx.doi.org/10.1016/j.bbadis.2013.08.004

Free radicals generated as a result of oxidative stress processes can be trapped by 5,5-dimethyl-1-pyrroline *N*-oxide (DMPO) to form DMPO-radical adducts, which can then be further tagged by IST, a method that utilizes an antibody against DMPO-adducts [2–5]. It would be of paramount importance if the formation of oxidation products could be assessed in vivo, allowing the study of specific cause–consequence relationships from specific oxidative events. This approach would allow scientists to correlate the detection of in situ oxidative stress markers with specific longitudinal pathological conditions associated with glioma tumor growth.

In a novel approach, we have combined the desired morphological image resolution of mMRI with a Gd-DTPA–albumin-based contrast agent for signal detection with the specificity of an antibody for DMPO nitrone adducts (anti-DMPO probe), to detect in vivo free radicals (see Fig. 1). In this study, the anti-DMPO probe was used to assess heterogeneous free-radical formation within orthotopic mouse gliomas.

2. Methods

2.1. Syntheses of DMPO-specific MRI contrast agents

To recognize the DMPO-radical adducts, a mouse monoclonal anti-DMPO antibody bound to a contrast agent was used. The macromolecular contrast material, biotin–BSA–Gd-DTPA, was prepared using a modification of the method of Dafni et al. [6]. The biotin moiety in the contrast material was added to allow histological localization. Biotin–BSA–Gd-DTPA was synthesized as described in Towner et al. [7]. A solution of biotin–BSA–Gd-DTPA was added directly to the solution of antibody (anti-DMPO, 200 μg/mL) for conjugation through a sulfo-NHS (N-succinimidyl-S-acetylthioacetate)–EDC (N-succinimidyl 3-(2-pyridyldithio)-propionate) link between albumin and antibody according to the protocol of Hermanson [8]. Sulfo-NHS was added to the solution of biotin–BSA–Gd-DTPA and EDC. This activated solution was added directly to the antibody (anti-DMPO, 20 μg/mL) for conjugation. The mixture was left to react for at least 2 h at 25 °C in the dark. The product was lyophilized and subsequently stored at 4 °C and reconstituted to the desired concentration for injections in phosphate buffer saline (PBS). The final amount of the product, anti-DMPO–biotin–BSA–Gd-DTPA (anti-DMPO probe), that was injected into the mice is estimated to be 20 μg anti-DMPO Ab/injection, and 10 mg biotin–BSA–Gd-DTPA/injection. The estimated molecular weight of the anti-DMPO–biotin–BSA–Gd-DTPA probe is estimated to be 232 kDa. As a control, normal mouse-IgG (obtained from a healthy mouse population; Alpha Diagnostic International, San Antonio, TX, USA) conjugated to biotin–BSA–Gd-DTPA (control IgG contrast agent) was synthesized by the same protocol to generate an isotype contrast agent.

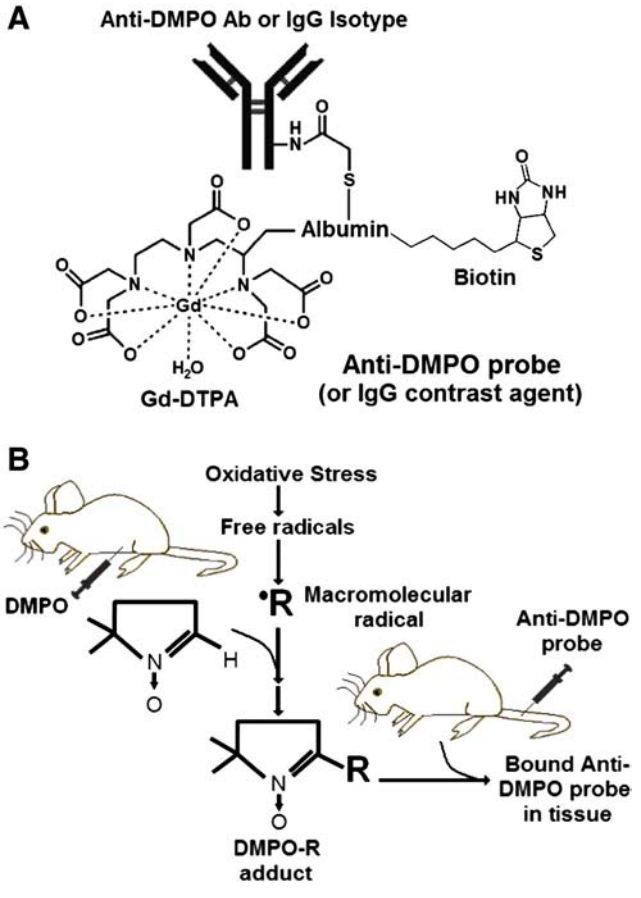

Fig. 1. Approach for combined in vivo mMRI and IST. (A) Anti-DMPO–albumin–Gd-DTPA–biotin mMRI probe (anti-DMPO probe). (B) Immuno-spin trapping of free radicals (•R) with anti-DMPO mMRI probe. DMPO is injected i.p. to trap free radicals and generate nitrone-radical (R) adducts. Anti-DMPO is injected i.v. to target nitrone-R adducts, which can be visualized by mMRI.

2.2. In vitro characterization of anti-DMPO probe

Vials were prepared containing either GL261 mouse glioma cells (10^6) alone, GL261 cells with hydrogen peroxide (H_2O_2) and DMPO, GL261 cells with DMPO + anti-DMPO probe, GL261 cells with H_2O_2 + DMPO + anti-DMPO probe, or water (no cells). Cells (mouse GL261 cells) were grown in flasks in complete growth medium (DMEM Media with 10% fetal bovine serum (FBS), Invitrogen, Grand Island, NY, USA) to confluency. Two to three hours before treatment, the growth medium was replaced with serum-free medium. DMPO (40 mM) was added to appropriate vials, and after 15 min equilibrium, H_2O_2 (50 μM) was added. In the samples that contained all components, the anti-DMPO probe was added (2 μg, based on antibody calculation), and cells were incubated for 45 min. Following incubation, cells were collected, washed with PBS, centrifuged (500 rpm), and the pellet was resuspended in PBS for MR imaging. Each measurement was repeated 4 times per treatment group.

2.3. Animal experiments

All animal experiments were conducted in accordance with the National Institutes of Health animal use and welfare guidelines, and with the authorization of the Oklahoma Medical Research Foundation institutional animal ethics committee.

2.3.1. Intracranial mouse brain tumor model

As a model for orthotopic intracranial brain tumors, a GL261 mouse glioma model was used (n = 8). Mouse glioma cells (GL261) were implanted intracerebrally in C57BL6/J mice. The heads of anesthetized mice were immobilized (stereotaxic unit; Kopf Instruments, Tujunga, CA), and with aseptic techniques, a 1 mm burr hole was drilled in the skull 1 mm anterior and 2 mm lateral to the bregma on the left side. A 20 μL gas-tight Hamilton syringe was used to inject 2×10^4 GL261 cells (in 10 μL of PBS) into the left frontal lobe at a depth of 1.5 mm relative to the dural surface in a stereotaxic unit. The cell lines were maintained and expanded immediately prior to inoculation. Following injection, the skin was closed with surgical sutures. The anti-DMPO probe was administered at 19 days following cell implantation. Mice (n = 4) were treated with DMPO for 3 days starting at day 16 following implantation of cells, and prior to the administration of the anti-DMPO probe. For an isotype contrast agent control, GL261 glioma-bearing mice (n = 4) were treated with DMPO, but were administered a non-specific mouse IgG-albumin–Gd-DTPA–biotin (IgG) contrast agent.

2.4. DMPO administration

DMPO (25 μL or 1.8 mM in saline; 125 μL volume) was administered i.p. 3× daily (every 6 h) for 3 days. DMPO administration started at day 16 following intracerebral implantation of GL261 glioma cells.

2.5. Magnetic resonance techniques

MR experiments were carried out under general anesthesia (1–2% Isoflurane, 0.8–1.0 L/min O_2). MRI experiments were conducted on a Bruker Biospec 7.0 Tesla/30 cm horizontal-bore imaging spectrometer. Anesthetised (2% Isoflurane) restrained mice were placed in an MR-compatible cradle and inserted into a MR probe, and their brains were localized by MRI. Images were obtained using a Bruker S116 gradient coil (2.0 mT/m/A), a 72 mm quadrature multi-rung RF coil, and mouse surface head coil. Mouse brains were imaged in vivo at various intervals (at 7, 10 and 14 days following cell implantation prior to administration of the anti-DMPO probe at day 21) and tumors as small as 0.05 mm in diameter could be detected. Multiple brain ^{1}H MR image slices were taken in the transverse plane using a spin echo multislice sequence (repetition time (TR) 0.8 s, echo time (TE) 23 ms, 128 × 128 matrix, 4 steps per acquisition, 3 × 4 cm^2 field of view, 1 mm slice thickness). Mouse brains were imaged at 0 (pre-contrast), 20, 40, 60, 120 and 180 min intervals post-probe or -contrast agent injection. Mice were injected intravenously with anti-DMPO or non-immune-IgG antibodies tagged with a biotin–Gd-DTPA–albumin-based contrast agent (200 μL/kg; 1 mg antibody/kg; 0.4 mmol Gd^{+3}/kg) [7]. T_1-weighted images were obtained using a variable TR (repetition time) RARE sequence (TR 200, 400, 800, 1200 and 1600 ms; TE 15 ms, FOV 2 × 2 cm^2, matrix 256 × 256, slice thickness 0.5 mm, 2 slices, and 2 steps per acquisition). Pixel-by-pixel relaxation maps were reconstructed from a series of T_1-weighted images using a nonlinear two-parameter fitting procedure. The T_1 relaxation value of a specified region-of-interest (ROI) was computed from all the pixels in the ROI by the following equation [9] (processed by ParaVision 4.0, Bruker): $S(TR) = S_0(1 - e^{-TR/T1})$, where TR is the repetition time (units: ms), S_0 is the signal intensity (integer machine units) at $TR \gg T_1$ and $TE = 0$, and T_1 is the constant of the longitudinal relaxation time (units: ms). Relative probe (contrast agent) concentrations, C (units: M), were calculated for each of the selected ROIs using the following formula [9]: $C \propto [1/T_1(\text{after}) - 1/T_1(\text{before})]$, where $1/T_1$ (after) is the T_1 rate taken at different time points after injection of probes, and $1/T_1$ (before) is the T_1 rate taken before injection of probes.

2.6. Excised brain tissues

Cardiac perfusion with PBS was performed while the mice were under anesthesia (Isoflurane), and then the heads were cut off using a guillotine. The skin and the muscles were removed from the head. Then the bones on the top of the head were carefully removed, from the cerebellum to the olfactory bulb through the bregma, and from one side of the head to the other side. The ear bones were carefully extracted from the brain; the optic chiasm and the olfactory bulb were excised in order to extract the brain. A transverse cut was then performed to get samples for fluorescence microscopy/immunohistochemistry (IHC) analyses or biochemical (ELISA [enzyme linked immunosorbent assay]) assays in the glioma and normal brain regions.

2.7. Immunohistochemistry

For fluorescence microscopy/IHC assessments, the brains were excised, and they were cut and fixed in Z-fixative (Zinc Formalin: Formaldehyde 3.7%, Zinc Sulfate). The tissues were then washed with PBS and incubated with 15% sucrose before embedding in Optimal Cutting Temperature (O.C.T.) compound and frozen in liquid nitrogen. Immunohistochemisty (IHC) staining of DMPO-nitrone adducts was done by incubating tissue sections with anti-DMPO antibodies conjugated to Cy3 in phosphate-buffered saline containing 0.1% v/v saponin. To target the Gd-based anti-DMPO probe in excised fixed tissues, cryosections were stained with either streptavidin-FITC (fluorescein isothiocyanate) or Cy3-labeled streptavidin (Jackson Immuno Research Labs, West Grove, PA, USA), which can bind to the biotin moiety of the albumin–Gd-DTPA–biotin contrast agent within the target tissue. For IHC staining of 3-nitrotyrosine (3-NT), a rabbit anti-nitrotyrosine antibody (Sigma, St. Louis, MO, USA) was used. For IHC staining of 4-hydroxy-2-nonenal (4-HNE), a rabbit anti-HNE antibody (Alpha Diagnostic International, San Antonio, TX, USA) was used. For fluorescence imaging of 3-NT or 4-HNE IHC a donkey anti-rabbit FITC secondary antibody (Jackson Immuno Research Laboratories) was used. Stained tissue slices were examined with a Nikon C1 confocal laser scanning microscope (Nikon Instruments, USA).

2.8. Tissue homogenates for oxidation assays

For preparation of tissue homogenates for ELISA assays, tissue samples were rinsed with PBS, homogenized in PBS and stored overnight at −20 °C. After two freeze–thaw cycles were performed to break cell membranes, the homogenates were centrifuged for 5 min at 5000 ×*g* (2–8 °C). The supernatants were removed immediately and assayed. Protein concentrations were measured using a Pierce(R) Microplate BSA (bicinchoninic acid) Protein Assay Kit (Pierce Biotechnology, Rockford, IL, USA) using BSA as a standard.

2.9. Lipid oxidation

The OxiSelect™ MDA adduct ELISA kit (Cell Biolabs, Inc., San Diego, CA, USA) was used for detection and quantification of MDA (malondialdehyde)-protein adducts in ex vivo mouse GL261 glioma and normal brain tissues as a measure of lipid peroxidation, similar to a study by El Ali et al. [10]. In brief, BSA (bovine serum albumin) standards and protein samples (10 μg/mL) were adsorbed onto a 96-well plate for 2 h at 37 °C. Then the MDA-protein adducts present in the sample or standard were probed with an anti-MDA antibody, followed by an HRP (horseradish peroxidase) conjugated secondary antibody. The quantity of MDA adduct in protein samples was determined by comparing its absorbance (at 450 nm) with that of a known MDA–BSA standard curve.

2.10. Protein oxidation

The OxiSelect™ Nitrotyrosine ELISA kit (Cell Biolabs, Inc., San Diego, CA, USA) was used for detection and quantification of 3-nitrotyrosine (3-NT) in protein samples from mouse GL261 and normal brain tissue lysates as a measure of protein oxidation. This nitrotyrosine quantification kit was a competitive ELISA. In brief, the unknown protein nitrotyrosine samples or nitrated BSA standards were first added to a nitrated BSA pre-absorbed EIA (enzyme immunoassay) plate. After a brief incubation, an anti-nitrotyrosine antibody was added, followed by an HRP conjugated secondary antibody. The protein nitrotyrosine content in unknown samples was determined by comparing with a standard curve that was prepared from predetermined nitrated BSA standards.

2.11. Statistical analyses

Statistical differences between the probe-administered and control groups were analyzed with an unpaired, two-tailed Student *t* test using commercially available software (InStat; GraphPad Software, San Diego, CA, USA). A p value of less than 0.05 was considered to indicate a statistically significant difference.

3. Results

3.1. Experimental strategy

Fig. 1 illustrates the anti-DMPO and IgG isotype contrast agent construct design, and depicts the experimental strategy for the in vivo IST-mMRI studies. An anti-body–albumin–Gd-DTPA–biotin construct was used for both the anti-DMPO probe and the non-specific IgG contrast agent isotype control. Initially, glioma-bearing mice were injected (i.p.) with DMPO consecutively for 5 days (3 times daily) to trap free radicals in glioma tissue, and then a tail-vein catheter was used to obtain molecular MR images of trapped DMPO-radical adducts that remained in glioma tissue in glioma-bearing mice with an anti-DMPO probe.

3.2. Anti-DMPO probe characterization in GL261 cells

Fig. 2 presents in vitro data regarding the effect of the anti-DMPO probe on MRI signal intensity (SI) and T_1 relaxation in oxidized GL261 glioma cells. GL261 cells that were oxidized with hydrogen peroxide, subsequently administered DMPO to trap free radicals, and then exposed to the anti-DMPO probe, were found to have an increased MR signal intensity and a corresponding decrease in T_1 relaxation time, compared to cells alone or oxidized cells with DMPO but without the anti-DMPO probe. GL261 cells administered DMPO and the anti-DMPO without hydrogen peroxide also had an increased SI and corresponding decrease in T_1 relaxation, and were found to be significantly different to vials containing GL261 cells + hydrogen peroxide + DMPO or water alone, but not GL261 cells alone.

3.3. In vivo detection of free radicals in GL261 gliomas

Fig. 3 depicts increased uptake of the anti-DMPO probe in glioma tissue (Fig. 3A). By comparison, a non-specific IgG contrast agent was not taken up in glioma tissue (Fig. 3B). GL261 glioma-bearing mice administered the anti-DMPO probe were found to have significantly increased changes in T_1 relaxation (Fig. 3C; $p < 0.001$) and MR SI (Fig. 3D; $p < 0.001$) in tumor regions compared to GL261 glioma-bearing mice administered a non-specific IgG Gd-based contrast agent. The anti-DMPO probe was also found to be significantly higher ($p < 0.001$) in tumor vs. contralateral tissues (Fig. 3C,D).

3.4. Confirmation of presence of anti-DMPO in ex vivo GL261 glioma tissue and co-localization with oxidative stress markers

A representative MR image (T_2-weighted) is shown in Fig. 4A, with a histological image in a tumor region with necrosis (Fig. 4B). Fluorescence detection of the anti-DMPO probe was found to be elevated in ex vivo glioma tissue (Fig. 4C). The fluorescence agent Cy3 (green) attached to streptavidin targets the biotin moiety of the anti-DMPO probe that is present in ex vivo excised tumor tissue from a GL261 glioma-bearing mouse administered the anti-DMPO probe in vivo. Comparatively, there wasn't any specific uptake of the IgG contrast agent in gliomas administered the isotype control complex (Fig. 4D).

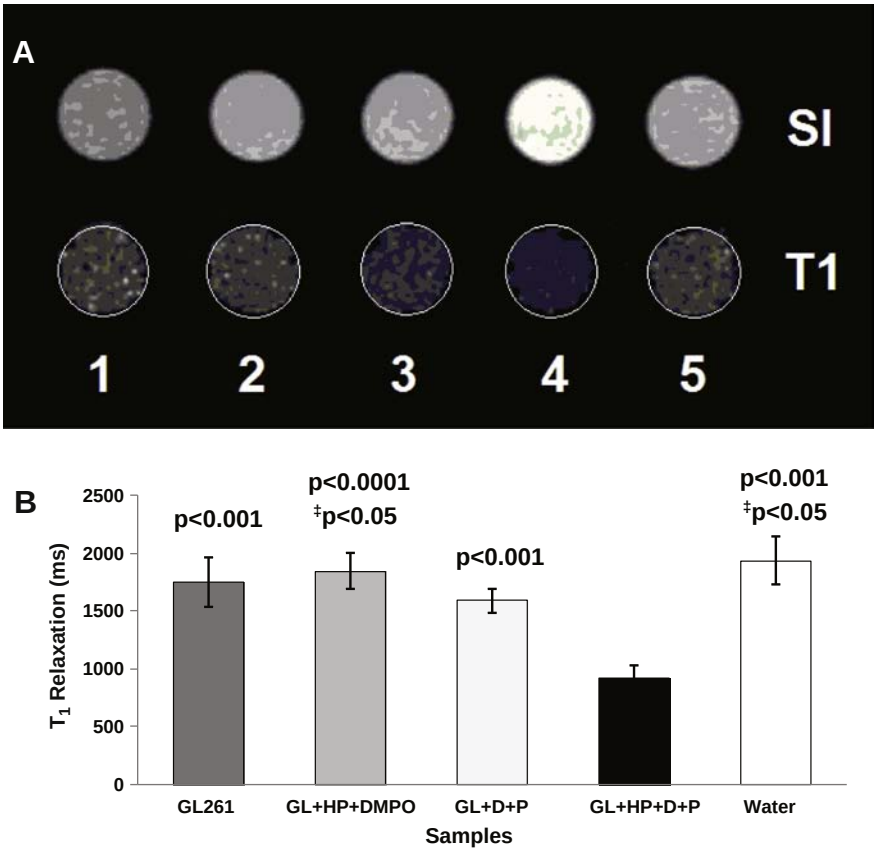

Fig. 2. In vitro assessment of the anti-DMPO probe in mouse GL261 glioma cells. (A) MRI signal intensities (SI) (T_1-weighted) and T_1 maps (T1) of vials (4 replicates for each) containing either (1) GL261 cells alone (in PBS), (2) GL261 cells + hydrogen peroxide (H_2O_2, abbreviated here as HP) + DMPO (GL + HP + DMPO), (3) GL261 cells + DMPO + anti-DMPO probe (GL + D + P), (4) GL261 cells + HP + DMPO + anti-DMPO probe (GL + HP + D + P), or (5) water (no cells). (B) Quantification of T_1 relaxation values (ms) from vials containing samples 1–5 described above. Values are represented as mean ± S.D. There was a significant decrease in T_1 relaxation for samples containing GL261 cells + HP + DMPO + anti-DMPO probe compared to GL261 cells alone ($p < 0.001$), GL261 cells with HP and DMPO ($p < 0.0001$), GL261 cells with DMPO + anti-DMPO probe ($p < 0.001$), or water ($p < 0.001$). There was also a significant decrease in T_1 relaxation for samples containing GL261 cells + DMPO + anti-DMPO probe compared to GL261 cells with HP and DMPO ($^{‡}p < 0.05$), or water ($^{‡}p < 0.05$), but not GL261 cells alone.

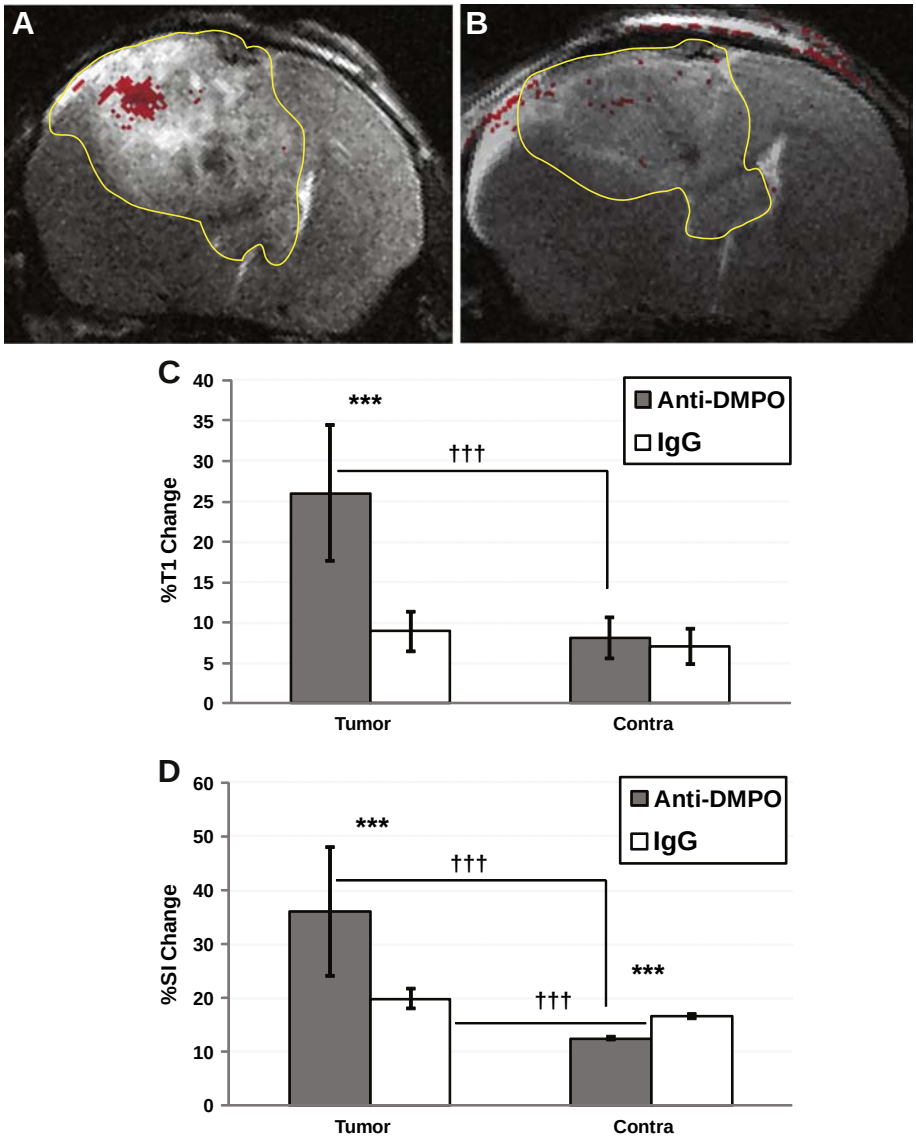

Fig. 3. mMRI detection of membrane-bound radical adducts in a GL261 mouse glioma model. (A) T_2-weighted MR image with an overlaid difference threshold image (depicted as a red region) (120 min post- and pre-administration of anti-DMPO probe) following administration of the anti-DMPO probe, taken at 30 days after intracerebral implantation of GL261 cells in mice (n = 4). Note increased uptake of the anti-DMPO probe in the peripheral tumor region surrounding a necrotic lesion (depicted as a dark void). (B) T_2-weighted MR image with an overlaid difference threshold image (120 min post- and pre-administration of the IgG contrast agent) following administration of the IgG contrast agent, taken at 27 days after intracerebral implantation of GL261 cells in mice (n = 4). Note no specific uptake of the IgG contrast agent in the tumor region. (C) Histogram of quantitative percent T_1 changes in tumor and contralateral (Contra) regions of GL261 glioma-bearing mice administered either the anti-DMPO probe (Anti-DMPO) or a non-specific IgG contrast agent (IgG). (D) Histogram of quantitative percent MR signal intensity (SI) changes in tumor and contralateral (Contra) regions of GL261 glioma-bearing mice administered either the anti-DMPO probe (Anti-DMPO) or a non-specific IgG contrast agent (IgG).

Co-localization (depicted as orange regions) of the anti-DMPO probe was also obtained for oxidative stress markers 3-NT (Fig. 4E) and 4-HNE (Fig. 4F) in some areas of glioma tissue from GL261 glioma-bearing mice administered DMPO and the anti-DMPO probe.

3.5. Confirmation of the presence of DMPO-trapped radicals in GL261 gliomas

GL261 glioma tissue from animals not administered the anti-DMPO probe, but given DMPO, was assessed for the immunohistochemical or ex vivo IST detection of DMPO-radical adducts. There was a detected increase in level of IHC-stained DMPO nitrone adducts from ex vivo glioma tissue (Fig. 5Ai and the increased magnification image in Aii), compared to normal brain tissue (Fig. 5Bi and Bii).

3.6. Detection of oxidized lipids and proteins in GL261 gliomas

Oxidized lipids (as commonly occurs with lipid peroxidation), measured by elevated malondialdehyde (MDA) protein adducts (pmol/mg tissue protein) were found to be significantly increased in ex vivo GL261 glioma homogenates ($p < 0.001$) compared to normal mouse brain tissue (Fig. 6A). Also 3-nitrotyrosine (3-NT) levels (nM/m tissue protein), an indication of oxidized proteins, were found to be significantly increased in ex vivo GL261 glioma tissue ($p < 0.05$) compared to normal brain tissue (Fig. 6B).

4. Discussion

After DMPO is administered, it binds to radicals to form radical adducts. It is thought that predominantly only radical adducts that are

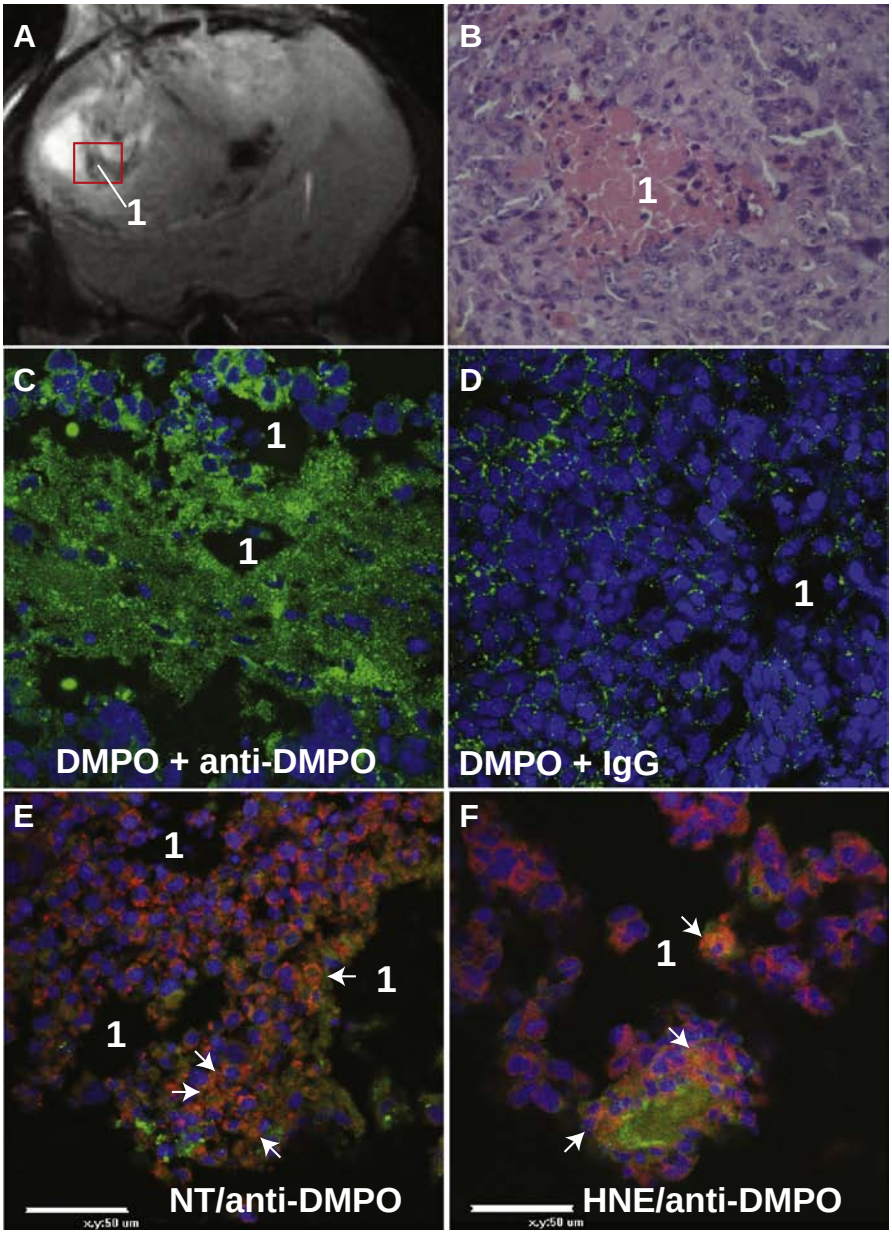

Fig. 4. Ex vivo detection of the anti-DMPO probe and co-localization with oxidative stress markers. (A) Representative T_2-weighted MR image of a GL261 glioma-bearing mouse brain, with a marked region (red rectangle) depicting where a histology (H&E) slide (B) was obtained in a region with necrosis (×400 magnification). (C) Fluorescence image of streptavidin-FITC (green) targeting the biotin moiety of the anti-DMPO probe in a GL261 glioma-bearing mouse. (D) Fluorescence image of streptavidin-FITC (green) which binds to the biotin moiety of the IgG contrast agent in a GL261 glioma-bearing mouse. Note that fluorescence levels are elevated in a GL261 mouse administered the anti-DMPO probe (C), but not the one administered the non-specific IgG contrast agent (D). Immunohistochemistry images of 3-NT (E) or 4-HNE (F) (both green) co-localized with the presence of the anti-DMPO probe (red, streptavidin-Cy3) in GL261 glioma-bearing mice administered DMPO and the anti-DMPO probe. Note co-localized areas with both anti-DMPO probe and either 4-HNE or 3-NT (orange, arrows used to depict some examples). Representative necrotic areas in panels A–E are labeled with the number 1. Cell nuclei are stained blue (Dapi). Magnification bars are 50 μm.

membrane-associated (e.g. protein and/or lipid radical adducts) will be targeted by the Gd-based anti-DMPO probe (~232 kDa) and detected by MRI. From another study using a similar probe construct to detect in vivo levels of inducible nitric oxide synthase (iNOS), transmission electron microscopy (TEM) was used to demonstrate that iNOS was detected within the plasma membrane in C6 rat glioma cells, and that an anti-iNOS probe was able to detect in vivo levels of iNOS specifically in glioma tissue [11]. Since the detected iNOS was within the plasma membrane, it was speculated that some of the anti-iNOS probe was internalized into the plasma membrane to allow mMRI detection. Whether the probe construct is internalized intracellularly would still need to be established in future studies.

mMRI relies on the specific labeling of extracellular cell surface receptors or antigens with a targeted contrast agent. The MRI contrast agent probe is targeted to a specific receptor or antigen by an antibody (Ab). These compounds alter proton magnetization relaxation times at their sites of accumulation, making them ideal for diagnostic purposes. Paramagnetic gadolinium (Gd)-based MR contrast agents generate a positive signal contrast (T_1 contrast) which enhances MR signal intensities of water molecules that surround these agents in T_1-weighted MR images. Gadolinium (Gd)-based probes that bind to affinity molecules, have recently become popular when used with mMRI. Our laboratory has previously used mMRI methodology to provide in vivo evidence regarding the over-expression of various tumor markers [7,11–14] in

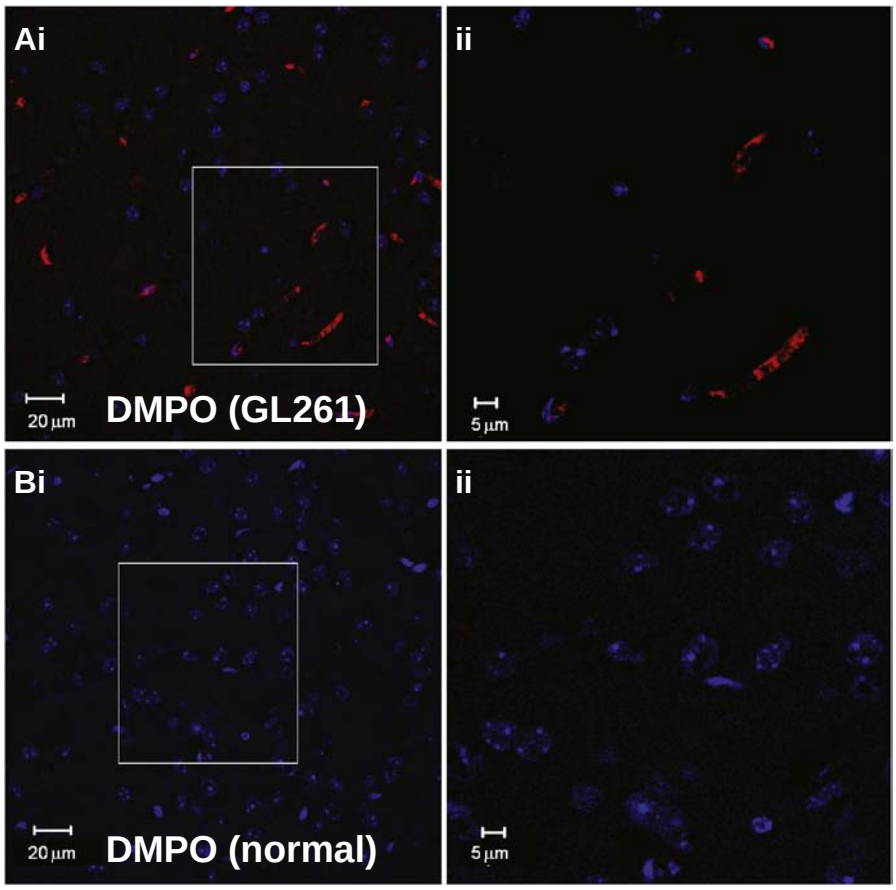

Fig. 5. Ex vivo detection of DMPO nitrone adducts in GL261 gliomas. Immunohistochemistry or IST images of DMPO-adducts from excised brain tissues of either a GL261 glioma-bearing mouse (Ai, and increased magnification image in Aii), or a normal mouse (Bi, and increased magnification image in Bii), both administered DMPO (no anti-DMPO probe). Enlarged images shown in (ii) are taken from regions outlined in corresponding (i) images. Note elevated DMPO-adducts in the GL261 glioma (compared to normal brain tissue). Magnification bars in images labeled "i" are 20 μm, and 5 μm for images labeled "ii".

glioma models. We have previously shown in rat glioma models (orthotopic C6 or RG2 gliomas) that the blood–brain-barrier is disrupted allowing the albumin-Gd-based probes to enter glioma tissue [11]. In the GL261 mouse model, it has been shown that there is BBB disruption, as revealed by confocal imaging of IgG leakage into tumor tissue and surrounding brain parenchyma [15]. Due to the leaky BBB in gliomas we have used a similar molecular imaging probe construct in other glioma models to detect c-Met [7] and iNOS [11]. It is anticipated that the low MW of DMPO (113.2) would also be able to reach the tumor via a leaky BBB. Recently we used the same anti-DMPO probe used in this study to assess radical formation in various tissues/organs (e.g. liver, lungs and kidneys) within diabetic mice [16], indicating the broad application of the anti-DMPO probe and mMRI in other oxidative-stress-related diseases.

Gliomas comprise the majority of primary brain tumors diagnosed annually in the United States (CBTRUS, 2011). Gliomas are classified by the World Health Organization according to their morphologic characteristics into astrocytic, oligodendroglial, and mixed tumors [17]. Approximately 15,000 patients die with glioblastomas in the U.S.A. per year [18]. Due to the infiltrative nature of gliomas, surgery is rarely effective, i.e. after surgical removal tumors recur predominantly within 1 cm of the resection cavity [19]. Despite modern diagnostics and treatments the median survival time for patients with glioblastomas does not exceed 15 months [19,20]. Prognosis is related not only to tumor grade but to glioma subtype, i.e. oligodendrogliomas are characterized by a better prognosis [17]. Other important hallmarks of malignant gliomas are their invasive behavior and angiogenesis [19].

Oxidative stress plays a major role in the growth of gliomas. For instance, the antioxidant status of glioma patients was found to be lowered [21]. It has also been suggested that there is a link between free radical generation and intra-mitochondrial cytochrome-c degradation, which could lead to the impairment of the apoptotic cytochrome-c-dependent cascade [22]. In addition it has been found that manganese superoxide dismutase is over-expressed in most brain tumors, leading to the increased activation of mitogen-activated protein kinases and phosphatidylinositol-3-kinases, which promote migration and invasion in glioma cells [23]. Oxidative modification of cell lipids and proteins also has potential consequences for tumor cell proliferation [24]. In this study, we detected in vivo elevated free radicals within mouse GL261 gliomas with the use of an anti-DMPO probe. It is hypothesized that major macromolecules, such as proteins and lipids, that are oxidized by free radicals generated in gliomas are targeted by the anti-DMPO probe. Supporting evidence of both oxidized lipids and proteins in GL261 gliomas was provided from quantitative ex vivo studies on GL261 glioma tissue, which indicated that there was significantly increased oxidized lipids (as measured by MDA-protein adducts) and proteins (as measured by 3-NT) in tumors compared to normal mouse brain tissue (Fig. 6). Qualitative co-localization of the anti-DMPO probe with 4-hydroxynonenal (HNE), another marker for oxidized lipids, or 3-NT, was detected in fluorescence images from glioma-bearing mice administered DMPO and the anti-DMPO probe (Fig. 4). Other investigators have shown that in ethylnitrosourea (ENU)-induced rat gliomas there are increased immunopositive histological regions for HNE, MDA and nitrotyrosine (3-NT) which correlate with glioma

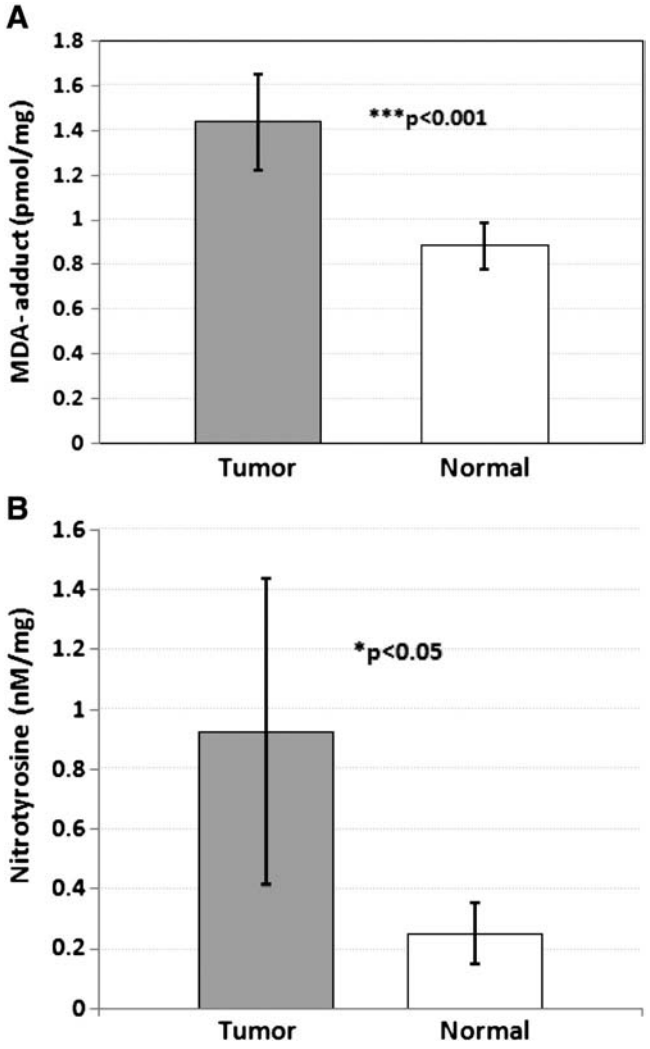

Fig. 6. Quantitative measure of the oxidation of macromolecules in ex vivo GL261 glioma tumors. (A) MDA-protein adduct concentration (pmol/mg protein) in tissue homogenates from mouse GL261 gliomas ($n = 8$) and normal brain ($n = 4$). There was a significant increase in MDA-adducts in GL261 mouse tumor tissue compared to normal brain samples (***$p < 0.001$). (B) 3-Nitrotyrosine (3-NT) concentration (nM/mg protein) in tissue homogenates from GL261 gliomas ($n = 6$) and normal brain ($n = 4$). There is a significant increase in 3-NT from GL261 gliomas compared to normal brain (*$p < 0.05$).

growth [25]. Our results strongly suggest that both oxidized lipids and proteins may be trapped by DMPO and subsequently detected by IST-mMRI detection with the anti-DMPO probe.

We also presented quantitative data supporting the increased affinity of the anti-DMPO probe for isolated GL261 glioma cells that were exposed to the ROS agent, hydrogen peroxide, and in the presence of DMPO and the anti-DMPO probe (Fig. 2), as well as GL261 cells exposed to both DMPO and the anti-DMPO probe without hydrogen peroxide. The exogenous hydrogen peroxide was added to ensure generation of free radicals in the in vitro environment, and verify specific binding of the anti-DMPO probe to glioma cells that generate free radicals. Addition of hydrogen peroxide to the GL261 cells in vitro did decrease T_1 relaxation 1.7-fold more-so compared to no addition of hydrogen peroxide. The in vitro results with hydrogen peroxide were similar to the in vivo results in glioma tissue where there was a 2.9-fold decrease in $\%T_1$ change. Perhaps in the in vivo tumor environment, hydrogen peroxide is being generated, which is being detected by DMPO trapping of hydroxyl radicals generated from hydrogen peroxide-mediated Fenton-like chemistry. It may be possible that endogenous hydrogen peroxide or subsequent free radicals generated from glioma cells in vitro may be dispersed in the cell culture media. It is interesting to point out that there is evidence that hydrogen peroxide is involved in the promotion of migration and invasion in glioma cells (U87) via manganese superoxide dismutase [23,26]. It has also been established that some glioma cell lines (e.g. U373MG) which have a mutated p53, are resistant to hydrogen peroxide induced cell death [27]. As related to this study, it should also be noted that mouse GL261 cells carry a point mutation in the p53 gene [28], allowing increased hydrogen peroxide to be produced which may play a role in the aggressive nature of these tumor cells.

Several studies have used IST in ex vivo tissues to detect DMPO-radical adducts [2,4,5]. Protein radicals trapped by DMPO to form DMPO-protein radical adducts, for example, were studied by Ramirez et al. [4] utilizing IST to detect oxidized-super oxide dismutase 1. Other studies also support increased lipid and protein oxidation in gliomas. Lipid peroxidation, as measured by increased levels of HNE-protein adducts by IHC, was found to be significantly increased in astrocytic (120 patient samples) and ependymal (40 samples) human glial tumors, and was proportionally elevated in tumors that were more malignant or had increased neovascularization [29]. HNE levels are found to be elevated in high-grade astrocytomas and glioblastomas [30,31]. HNE levels are particularly important as this signaling molecule is known to act as a growth-regulating factor [30].

An advantage of the IST approach coupled with mMRI is that heterogeneous tissues, such as tumors, can be studied to obtain spatial differences in the detection of free radical levels (detected by the presence of the anti-DMPO probe via coupling to DMPO-radical nitrone adducts). In this study, we were able to show that free radical adducts are mainly distributed in localized peripheral tumor regions near necrotic regions (Fig. 3A). In other studies on either rat F98 gliomas [32] or rat 9L gliosarcomas [33], positron emission tomography (PET) was used to demonstrate that increased ^{18}F-fluorodeoxy glucose (FDG) uptake was found to occur mainly in peripheral tumor regions. ^{18}F-FDG which is often used to study glucose uptake, has also previously shown an association with cell proliferation. For instance, ^{18}F-FDG has been found to be a suitable marker to assess PI3K inhibitors, where the PI3K oncogenic signaling pathway is involved with the regulation of multiple cellular processes including glucose metabolism, proliferation and cell survival [34]. The ex vivo fluorescence data (Fig. 4) indicates that the anti-DMPO-probe is distributed mainly in tumor regions with increased cell proliferation surrounding necrotic lesions. Ex vivo IST of mice administered DMPO only, confirms the presence of DMPO-radical adducts in gliomas (Fig. 5).

There are other imaging methods that have been used to detect radicals, including ESR, fluorescence imaging or Overhauser-enhanced MRI (OMRI). OMRI potentially offers a potential method of detecting low concentrations of free radical species generated by specific biological processes; however spatial resolution and general radical detection are limited [35]. 3D-OMRI currently is mainly used to detect injected free radicals (1-oxyl-2,2,5,5-tetramethyl-2,5-dihydro-1H-pyrrole-3-carboxylic acid, or TOPCA), and this technique was used in rats bearing C6 brain-implanted gliomas [35]. Although ESR imaging is sensitive, it lacks the image resolution of MRI and is often limited to the detection of an injected paramagnetic probe at the injection site. However, it should be noted that this technique has been used to detect in vivo nitric oxide in ischemic tissues [36] and lipopolysaccharide exposed mice [37]. The disadvantage of fluorescence imaging is that it is restricted to excised tissues or isolated cells.

5. Conclusions

Here we used a combination of mMRI and IST to show for the first time the non-invasive in vivo quantitative detection of free radicals in mouse gliomas. Using both mMRI and IST provides the advantage of in vivo image resolution and spatial differentiation of regional events in heterogeneous tissues or organs and the regional targeting of free radical mediated oxidation of cellular components, such as

membrane-associated proteins and lipids. Qualitative fluorescence data for the presence of the anti-DMPO probe, as well as fluorescence IST data for the presence of DMPO-radical adducts, verifies that the in vivo approach is feasible. A correlation between the presence of the anti-DMPO probe and oxidized lipids or proteins also supports the ability of the anti-DMPO probe to detect free radical associated processes. This method can be applied towards any cancer for the in vivo assessment of macromolecular free radical levels.

Conflict of interest

The authors declare no competing financial interests.

Acknowledgements

Funding was obtained by the Oklahoma Medical Research Foundation (RAT) and the National Institute of Environmental Health Sciences (NIEHS) (RPM). We would like to thank Dr. Ting He for assisting with the GL261 mouse glioma model.

References

[1] A. Federico, F. Morgillo, C. Tuccillo, F. Ciardiello, C. Loguercio, Chronic inflammation and oxidative stress in human carcinogenesis, Int. J. Cancer 121 (2007) 2381–2386.
[2] R.P. Mason, Using anti-5,5-dimethyl-1-pyrroline N-oxide (anti-DMPO) to detect protein radicals in time and space with immune-spin trapping, Free Radic. Biol. Med. 36 (2004) 1214–1223.
[3] D.C. Ramirez, S.E. Gomez Mejiba, R.P. Mason, Mechanism of hydrogen peroxide-induced Cu, Zn-superoxide dismutase-centered radical formation as explored by immune-spin trapping: the role of copper- and carbonate radical anion-mediated oxidations, Free Radic. Biol. Med. 38 (2005) 201–214.
[4] D.C. Ramirez, S.E. Gomez-Mejiba, J.T. Corbett, L.J. Deterding, K.B. Tomer, R.P. Mason, Cu, Zn-superoxide dismutase-driven free radical modifications: copper- and carbonate radical anion-initiated protein radical chemistry, Biochem. J. 417 (2009) 341–353.
[5] C.D. Detweiler, L.J. Deterding, K.B. Tomer, C.F. Chignell, D. Germolec, R.P. Mason, Immunological identification of the heart myoglobin radical formed by hydrogen peroxide, Free Radic. Biol. Med. 33 (2002) 364–369.
[6] H. Dafni, L. Landsman, B. Schechter, F. Kohen, M. Neeman, MRI and fluorescence microscopy of the acute vascular response to VEGF165: vasodilation, hyperpermeability and lymphatic uptake, followed by rapid inactivation of the growth factor, NMR Biomed. 15 (2002) 120–131.
[7] R.A. Towner, N. Smith, Y. Tesiram, P. Garteiser, D. Saunders, R. Cranford, R. Silasi-Mansat, O. Herlea, L. Ivanciu, D. Wu, F. Lupu, *In vivo* detection of c-Met expression in a rat C6 glioma model, J. Cell. Mol. Med. 12 (2008) 174–186.
[8] G. Hermanson, Bioconjugate Techniques, Academic Press, New York, 1996. 456–493 (494–527).
[9] E.M. Haacke, R.W. Brown, M.R. Thompson, R. Venkatesan, Magnetic Resonance Imaging: Physical Principles and Sequence Design, Wiley-Liss, 1999.
[10] A. El Ali, T.R. Doeppner, A. Zechariah, D.M. Hermann, Increased blood–brain barrier permeability and brain edema after focal cerebral ischemia induced by hyperlipidemia: role of lipid peroxidation and calpain-1/2, matrix metalloproteinase-2/9, and RhoA overactivation, Stroke 42 (2011) 3238–3244.
[11] R.A. Towner, N. Smith, S. Doblas, P. Garteiser, Y. Watanabe, T. He, S. Saunders, O. Herlea, R. Silasi-Mansat, F. Lupu, *In vivo* detection of inducible nitric oxide synthase (iNOS) in rodent gliomas, Free Radic. Biol. Med. 48 (2010) 691–703.
[12] R.A. Towner, N. Smith, Y. Asano, S. Doblas, D. Saunders, Molecular MRI approaches used to aid in the understanding of the tissue regeneration marker Met *in vivo*: implications for tissue engineering, Tissue Eng. Part A 16 (2010) 365–371.
[13] R.A. Towner, N. Smith, Y. Asano, T. He, S. Doblas, D. Saunders, R. Silasi-Mansat, F. Lupu, C.E. Seeney, Molecular MRI approaches used to aid in the understanding of angiogenesis *in vivo*: implications for tissue engineering, Tissue Eng. Part A 16 (2010) 357–364.
[14] T. He, N. Smith, D. Saunders, S. Doblas, J. Hoyle, R. Silasi-Mansat, F. Lupu, M. Lerner, D.J. Brackett, R.A. Towner, Molecular MRI assessment of vascular endothelial growth factor receptor-2 in a rat C6 glioma model, J. Cell. Mol. Med. 15 (2011) 837–849.
[15] M. Reis, C.J. Czupalla, N. Ziegler, K. Devraj, J. Zinke, S. Seidel, R. Heck, S. Thom, J. Macas, E. Bockamp, M. Fruttiger, M.M. Taketo, S. Dimmeler, K.H. Plate, S. Liebner, Endothelial Wnt/β-catenin signaling inhibits glioma angiogenesis and normalizes tumor blood vessels by inducing PDGF-B expression, J. Exp. Med. 209 (2012) 1611–1627.
[16] R.A. Towner, N. Smith, D. Saunders, M. Henderson, K. Downum, F. Lupu, R. Silasi-Mansat, D.C. Ramirez, S.E. Gomez-Mejiba, M.G. Bonini, M. Ehrenshaft, R.P. Mason, *In vivo* imaging of immunospin-trapped radicals with molecular magnetic resonance imaging in a mouse diabetes model, Diabetes 61 (2013) 2405–2413.
[17] M. Sanson, J. Thillet, K. Hoang-Xuan, Molecular changes in gliomas, Curr. Opin. Oncol. 16 (2004) 607–613.
[18] Central Brain Tumor Registry of the United States (CBTRUS), 2011 CBTRUS Statistical Report: Primary Brain and Central Nervous System Tumors Diagnosed in the United States in 2004–2007, 2011.
[19] T. Demuth, M.E. Berens, Molecular mechanisms of glioma cell migration and invasion, J. Neurooncol. 70 (2004) 217–228.
[20] R.D. Rao, C.D. James, Altered molecular pathways in gliomas: an overview of clinically relevant issues, Semin. Oncol. 31 (2004) 595–604.
[21] S. Kandavelu, A.J. Vanisree, A study on the biochemical and cytogenetic status in the blood of glioma patients, Pak. J. Biol. Sci. 14 (2011) 511–518.
[22] L. Macchioni, M. Davidescu, M. Sciaccaluga, G. Marchetti, S. Coaccioli, R. Roberti, L. Corazzi, E. Castigli, Mitochondrial dysfunction and effect of antiglycolytic bromopyruvic acid in GL15 glioblastoma cells, Lab. Invest. 91 (2011) 1766–1776.
[23] F. Li, H. Wang, C. Huang, J. Lin, G. Zhu, R. Hu, H. Feng, Hydrogen peroxide contributes to the manganese superoxide dismutase promotion of migration and invasion in glioma cells, Free Radic. Res. 45 (2011) 1154–1161.
[24] C. Rice-Evans, R. Burdon, Free radical–lipid interactions and their pathological consequences, Prog. Lipid Res. 32 (1993) 71–110.
[25] M.A. Mahlke, L.A. Cortez, M.A. Ortiz, M. Rodriguez, K. Uchida, M.K. Shigenaga, S. Lee, Y. Zhang, K. Tominaga, G.B. Hubbard, Y. Ikeno, The anti-tumor effects of calorie restriction are correlated with reduced oxidative stress in ENU-induced gliomas, Pathobiol. Aging Age Relat. Dis. 1 (2011) 7189.
[26] F. Li, T. Chen, S. Hu, J. Lin, R. Hu, H. Feng, Superoxide mediates direct current electric field-induced directional migration of glioma cells through the activation of AKT and ERK, PLoS One 8 (4) (2013) e61195.
[27] K. Datta, P. Babbar, T. Srivastava, S. Sinha, P. Chattopadhyay, p53 dependent apoptosis in glioma cell lines in response to hydrogen peroxide induced oxidative stress, Int. J. Biochem. Cell Biol. 34 (2002) 148–157.
[28] T. Szatmári, K. Lumniczky, S. Désaknai, S. Trajcevski, E.J. Hidvégi, H. Hamada, G. Sáfrány, Detailed characterization of the mouse glioma 261 tumor model for experimental glioblastoma therapy, Cancer Sci. 97 (2006) 546–553.
[29] G. Juric-Sekhar, K. Zarkovic, G. Waeg, A. Cipak, N. Zarkovic, Distribution of 4-hydroxynonenal–protein conjugates as a marker of lipid peroxidation and parameter of malignancy in astrocytic and ependymal tumors of the brain, Tumori 95 (2009) 762–768.
[30] K. Zarkovic, G. Juric, G. Waeg, D. Kolenc, N. Zarkovic, Immunohistochemical appearance of HNE–protein conjugates in human astrocytomas, Biofactors 24 (2005) 33–40.
[31] A. Zajdel, A. Wilczok, J. Slowinski, J. Orchel, U. Marurek, Aldehydic lipid peroxidation products in human brain astrocytomas, J. Neurooncol 84 (2007) 167–173.
[32] D. Mathieu, R. Lecomte, A.M. Tsanaclis, A. Larouche, D. Fortin, Standardization and detailed characterization of the syngeneic Fisher/F98 glioma model, Can. J. Neurol. Sci. 34 (2007) 296–306.
[33] C.S. Dence, D.E. Ponde, M.J. Welch, J.S. Lewis, Autoradiographic and small-animal PET comparisons between (18)F-FMISO, (18)F-FDG, (18)F-FLT and the hypoxic selective (64)Cu-ATSM in a rodent model of cancer, Nucl. Med. Biol. 35 (2008) 713–720.
[34] C.J. Kelly, K. Hussien, R.J. Muschel, 3D tumor spheroids as a model to assess the suitability of [18F]FDG-PET as an early indicator of response to PI3K inhibition, Nucl. Med. Biol. 39 (2012) 986–992.
[35] P. Massot, E. Parzy, L. Pourtau, P. Mellet, G. Madelin, S. Marque, J.M. Franconi, E. Thiaudiere, *In vivo* high-resolution 3D Overhauser-enhanced MRI in mice at 0.2 T, Contrast Media Mol. Imaging 7 (2012) 45–50.
[36] P. Kuppusamy, R.A. Shankar, V.M. Roubaud, J.L. Zweier, Whole body detection and imaging of nitric oxide generation in mice following cardiopulmonary arrest: detection of intrinsic nitrosoheme complexes, Magn. Reson. Med. 45 (2001) 700–707.
[37] T. Yoshimura, H. Yokoyama, S. Fujii, F. Takayama, K. Oikawa, H. Kamada, *In vivo* EPR detection and imaging of endogenous nitric oxide in lipopolysaccharide-treated mice, Nat. Biotechnol. 14 (1996) 992–994.